NASA Technical Memorandum 4099

Estimation of Longitudinal Stability and Control Derivatives for an Icing Research Aircraft From Flight Data

James G. Batterson and Thomas M. O'Mara

MARCH 1989

NASA

NASA Technical Memorandum 4099

Estimation of Longitudinal Stability and Control Derivatives for an Icing Research Aircraft From Flight Data

James G. Batterson
Langley Research Center
Hampton, Virginia

Thomas M. O'Mara
The George Washington University
Joint Institute for Advancement of Flight Sciences
Langley Research Center
Hampton, Virginia

National Aeronautics and
Space Administration
Office of Management
Scientific and Technical
Information Division

1989

Summary

The National Aeronautics and Space Administration, at its Lewis Research Center, develops and coordinates plans and results related to icing computer-code predictions, icing research tunnel (IRT) measurements, and icing research flights. To allow for the comparison of research flight results with icing code predictions and IRT measurements, Lewis has collaborated with the NASA Langley Research Center for the planning and analysis of a series of icing research flights related to the determination of stability and control derivatives from research flight data.

This paper presents the results of applying a modified stepwise regression algorithm and a maximum likelihood algorithm to flight data from a twin-engine commuter-class icing research aircraft. The results are in the form of body-axis stability and control derivatives related to the short-period, longitudinal motion of the aircraft. Data were analyzed for the baseline aircraft ("uniced") and for the aircraft with an artificial glaze-ice shape attached to the leading edge of the horizontal tail. The results are discussed as to the accuracy of the derivative estimates and the difference between the derivative values found for the baseline and the "iced" aircraft. Additional comparisons are made between the maximum likelihood results and the modified stepwise regression results with causes for any discrepancies postulated.

Introduction

The known dangers to safe flight that are caused by the accumulation of ice on aircraft components have given rise to a multifaceted approach to understanding the causes and predicting the effects of aircraft icing (ref. 1). The National Aeronautics and Space Administration (NASA), at its Lewis Research Center (LeRC), supports an Icing Technology Project Office in which plans and results related to icing computer-code predictions, icing research tunnel (IRT) measurements, and icing research flights are coordinated. To allow for the comparison of research flight results with icing code predictions and IRT measurements, LeRC has collaborated with the NASA Langley Research Center (LaRC) for the planning and analysis of a series of icing research flights related to the determination of stability and control derivatives from research flight data.

The successful estimation of stability and control derivatives from flight data has two important ramifications. First, the values for the derivatives can be compared with values derived from the analytical icing codes and from the IRT. These comparisons allow for an assessment of the confidence that should be put in analytical predictions and wind-tunnel results as they relate to an aircraft in flight. Second, flight-derived derivatives can be used judiciously along with those provided by analytical predictions and wind-tunnel tests to upgrade simulator math models to provide a realistic set of aerodynamics for pilot-in-the-loop simulations of icing scenarios. Such simulations can provide definitive information on how any measured degradation of the aircraft flying qualities actually affects its handling qualities.

Previous work on the estimation of stability and control derivatives from flight tests for an iced aircraft has been performed by LeRC and Kohlman Systems Research, Inc. (KSR), as reported in references 2 and 3. That earlier work employed a modified maximum likelihood technique to estimate the stability and control derivative values. The accuracies of these stability and control derivatives were estimated by an approximation to the Cramer-Rao bound given by the maximum likelihood algorithm. Since it is known that the Cramer-Rao bound estimates indicate better accuracy than is actually achievable by repeated experiments (ref. 4), and since the earlier work showed small, but apparently discernible, differences in the derivative values for the "iced" versus "uniced" aircraft, the first phase of the LaRC plan was to determine the expected accuracy of the estimated derivative values. To this end an ensemble of 45 maneuvers was flown at the same flight condition. These maneuvers were then individually analyzed as to longitudinal stability and control derivatives using both a maximum likelihood (ML) algorithm and a stepwise regression (SR) algorithm. The ensemble standard deviation for the parameter estimates was compared with the average of the Cramer-Rao bound estimates (maximum likelihood) for the ensemble and the average estimate of standard error (stepwise regression). Maneuvers were then flown from constant-power, $1g$ flight at several trim airspeeds for both the uniced and artificially iced aircraft, and the recorded data from those maneuvers were analyzed for longitudinal stability and control derivatives using both a stepwise regression and a maximum likelihood algorithm. The flight test program also included several data compatibility maneuvers for the assessment of data quality and several deceleration/acceleration maneuvers for direct determination of lift and pitching-moment curves.

The purpose of this paper is to present the results of applying a modified stepwise regression algorithm (ref. 5) and a maximum likelihood algorithm (ref. 6) to flight data from a twin-engine, commuter-class icing research aircraft. The results are in the form of body-axis stability and control derivatives related to the short-period, longitudinal motion of

the aircraft. Data were analyzed for the baseline aircraft ("uniced") and for the aircraft with an artificial glaze-ice shape attached to the leading edge of the horizontal tail. The results are discussed as to the accuracy of the derivative estimates and the difference between the derivative values found for the baseline "uniced" and the "iced" aircraft. Additional comparisons are made between the maximum likelihood results and the modified stepwise regression results with causes for any discrepancies postulated. The paper is organized as follows: After this introduction, the aircraft, its instrumentation, and the flight test maneuvers will be briefly discussed followed by a section on the analysis techniques. The main part of the paper will then present the results of the data analysis followed by a section summarizing the conclusions to be drawn from these results.

Symbols

a_z	vertical acceleration, g units
b	wing span, m
b_{ax}	calculated constant bias in longitudinal-acceleration measurement, m/sec^2
b_{az}	calculated constant bias in vertical-acceleration measurement, m/sec^2
b_q	calculated constant bias in pitch-rate measurement, rad/sec
b_α	calculated constant bias in angle-of-attack measurement, rad
b_θ	calculated constant bias in pitch-angle measurement, rad
C_l, C_m, C_n	rolling-, pitching-, and yawing-moment coefficients, respectively
C_X, C_Y, C_Z	longitudinal-, lateral-, and vertical-force coefficients, respectively
$\bar{c}$	mean aerodynamic chord, m
g	acceleration due to gravity ($1g \approx 9.81$ m/sec^2)
I_X, I_Y, I_Z	moments of inertia about roll, pitch, and yaw axes, respectively, kg-m^2
I_{XZ}	product of inertia, kg-m^2
J_{ML}	cost function for maximum likelihood algorithm
J_{SR}	cost function for stepwise regression algorithm
m	aircraft mass, kg
N, n	number of data points
p, q, r	roll, pitch, and yaw rates, respectively, rad/sec or deg/sec
S	wing area, m^2
S_{XX}	total sum of squares (corrected for mean)
$s(\ )$	standard error
$\bar{s}(\ )$	average of standard errors given by program
$s_E(\ )$	ensemble-average standard error for a group of values
$t_{\alpha*/2,n-2}$	student t-distribution
u, v, w	longitudinal, lateral, and vertical velocity components, respectively, m/sec
V	total airspeed, $(u^2+v^2+w^2)^{1/2}$, m/sec
$x_j(i)$	measured aircraft response or control surface input
$y(i)$	computed aerodynamic coefficients
$y_0(x_0)$	linear approximation of $C_{m_{\delta_e}}$ corresponding to some x_0 value
z_j	measured output
$\hat{z}_j$	computed output
α	corrected (free-stream) angle of attack, rad or deg
α_M	experimentally measured angle of attack, rad or deg
α^*	criteria for achieving a desired prediction interval
β	angle of sideslip, rad or deg
$\delta_e, \delta_a, \delta_r$	elevator, aileron, and rudder deflection, respectively, rad or deg
Θ	aerodynamic stability or control parameters

Θ_0 constant offset term

Θ_i derivative with respect to ith response or control surface input

θ, ϕ pitch and roll angles, respectively, rad or deg

λ_α upwash (scale-factor) correction for angle of attack

ρ air density, kg/m^3

$\widehat{\sigma}_j^2$ variance estimate of measurement noise (eq. (2))

$C_{m_q} = \frac{\partial C_m}{\partial \frac{q\bar{c}}{2V}}$ $C_{Z_q} = \frac{\partial C_Z}{\partial \frac{q\bar{c}}{2V}}$

$C_{m_\alpha} = \frac{\partial C_m}{\partial \alpha}$ $C_{Z_\alpha} = \frac{\partial C_Z}{\partial \alpha}$

$C_{m_{\delta_e}} = \frac{\partial C_m}{\partial \delta_e}$ $C_{Z_{\delta_e}} = \frac{\partial C_Z}{\partial \delta_e}$

A dot over a symbol represents the derivative with respect to time.

Aircraft and Instrumentation

The icing research aircraft is a modified deHavilland DHC-6 Twin Otter. It is powered by two Pratt & Whitney PT6A-20A gas turbine engines. Physical characteristics for the aircraft are found in table I. A three-view drawing is presented in figure 1. Longitudinal control is effected by elevator and hydraulically actuated flaps; lateral and directional control, through ailerons and rudder, respectively. The elevator, ailerons, and rudder all have trim tabs.

The instrumentation, which was provided and installed by KSR, included three-axis orthogonal linear accelerometers, three-axis angular rate gyros, and three-axis attitude gyros. Angles of attack and sideslip were measured by balsa wood vanes installed on a nose boom. Elevator, rudder, and aileron positions were measured by potentiometers placed at the control surface.

Since flaps were set and remained constant during an entire series of maneuvers, flap position was given by a readout in the cockpit and was recorded by the flight engineer for future reference.

Data were recorded onboard at 20 samples per second; all channels were sampled within 1 msec by the KSR data acquisition system (DAS). Because of buffer limitations of the KSR system, only 24 sec of the 20-samples-per-second data could be obtained before the buffer contents had to be written onto a cassette tape. The write-off period was nominally 60 to 90 sec. Hence, maneuvers had to be flown within the 24-sec slot while retrimming and/or housekeeping could be done during the 60- to 90-sec write-off period.

Research personnel onboard the aircraft were the research pilot in the cockpit left seat, an observer in the cockpit right seat, and the flight test engineer in the cabin for operating the DAS and coordinating available 24-sec test slots with the pilot.

After each flight, the recorded data cassettes were sent to KSR where the data were reduced to engineering units. The engineering-units data were written by KSR to a nine-track magnetic tape which was sent to LaRC for stability and control analysis.

Research Flights

The four airplane configurations flown are given in the following table:

Configuration	Aircraft condition	Flap deflection	Flight designation
1	Baseline (uniced)	0°	88-5
2	Baseline (uniced)	10°	88-6
3	Artificial ice on tail	0°	88-7
4	Artificial ice on tail	10°	88-8

These flights were designated as 88-5, 88-6, 88-7, and 88-8, respectively, by LeRC. Within each of these flights, each 24-sec slice of individual maneuvers was assigned a run number. The aircraft is limited to 10° flaps in an icing environment as a safety precaution. The artificial ice was a styrofoam form modeled after moderate glaze ice that had previously been seen and carefully photographed during natural icing encounters and in the IRT. This shape was glued to an aluminum form that was contoured to the leading edge of the horizontal tail. The aluminum was secured to the leading edge by attaching straps to the stabilizer hinge line as shown in figure 2. Four types of maneuvers were flown in each configuration:

1. Data compatibility maneuvers
2. Small-amplitude longitudinal perturbations
3. Large-amplitude longitudinal perturbations
4. Deceleration/acceleration maneuvers

The data compatibility maneuvers involved exciting large angular rates about all axes, thus leading to large excursions in all Euler angles and to large variations in linear accelerations, airspeed, angle of attack, and angle of sideslip. These data were examined using the algorithm described in reference 7 to assess the quality of the DAS measurements. In these maneuvers, in which no attempt was made to

excite any of the aircraft modes, only the air data sensors, rate sensors, and linear accelerometers were exercised.

The small-amplitude maneuvers were initiated by elevator "2-1" doublets designed to excite the short-period longitudinal motion of the aircraft. An example of the control surface movement and aircraft longitudinal responses is given in figure 3. These maneuvers were planned to excite $\pm 0.3g$ of vertical acceleration. However, because of an erroneous accelerometer readout in the cockpit, these maneuvers were sometimes of amplitude $\pm 1.0g$ of vertical acceleration.

The large-amplitude perturbations were initiated by random elevator doublets superimposed on an otherwise monotonically increasing angle of attack. For these maneuvers, the pilot pulls steadily back on the stick over the 24-sec test window, interrupting the steady pull at random intervals to apply small elevator doublets. In this way a large angle-of-attack range can be probed in a single maneuver at a constant power setting.

The deceleration/acceleration maneuvers were performed by setting power for $1.0g$-level flight at 120 knots and then slowly pulling back on the stick, decelerating at about 2 knots/sec. Then, if time was available in the 24-sec test window, the pilot would push the stick forward again to accelerate at 2 knots/sec, eventually returning to the initial flight condition.

The small-amplitude maneuvers fell into two groups. In the first group, to ascertain the accuracy of the derivative estimates, a set of maneuvers was performed in which the aircraft was trimmed at an airspeed of approximately 120 knots, and a series of 45 small-amplitude longitudinal perturbations was executed. These 45 sets of small-amplitude maneuvers provided a statistically significant ensemble of maneuvers, each of which should produce the same derivative estimates. Analyzing each maneuver of this ensemble and calculating the mean and standard deviation for the 45 results for each of the longitudinal stability and control derivatives gives a measure of how much a parameter estimate might vary statistically between two maneuvers at the same flight condition.

In the second group, the rest of the small-amplitude maneuvers were performed at different airspeeds with one or two repeats at each airspeed. These maneuvers were analyzed for trends in the derivatives relative to flight condition. Because the effect of artificial ice on lift and drag of the whole aircraft should be small and because the aircraft was trimmed at different airspeeds using only the elevator tab (constant power), it was assumed that direct comparisons could be made between the clean and "iced" derivatives at each trim airspeed.

Data Analysis Methods

The raw engineering-units data are first corrected for all known instrumentation offsets from the aircraft center of gravity and for flow effects. Next, several maneuvers are analyzed with the maximum likelihood algorithm reported in reference 7 for the estimation of instrument biases and possible scale-factor errors. This process is known as data compatibility or data consistency checking. Once a data set is available, the identification process still has two remaining stages. The first stage is the determination of the parametric model structure. Then, the second stage is the estimation of the corresponding parameter values. The model structure was determined using a modified stepwise regression. This technique can determine significant terms among the candidate variables and estimate corresponding parameters. Each new variable chosen for entry into the regression equation is the one that has the largest correlation with the measured dependent variable (y) after adjusting for the effect on y of the variables already selected. This correlation is reflected by the calculated F-statistic of the variable. The selected parameters are estimated by minimizing the cost function

$$J_{\mathrm{SR}} = \sum_{i=1}^{N} \left[y(i) - \Theta_0 - \sum_{j=1}^{\ell} \Theta_j \, \Delta x_j(i) \right]^2 \qquad (1)$$

where $y(i)$ is the aerodynamic coefficient computed from measured data at time i, N is the number of data points, and $\ell + 1$ is the number of parameters (or independent variables) in the regression equation. At every step of the regression, the variables incorporated into the model in previous stages and the new variable entering the model are reexamined. Any variable that provides a nonsignificant contribution (due to correlation with more recently added terms) is removed from the model. The process of selecting and checking variables continues until no more are admitted to the equation and no more are rejected. Experience shows, however, that the model based only on the significance of individual parameters in the model equation can still include too many terms and, therefore, may have poor prediction capabilities (ref. 8). Therefore, several criteria for the selection of an adequate model were introduced in reference 8. Details of this model-structure determination procedure are also explained in that reference.

Finally, each model and each maneuver were analyzed by the maximum likelihood (ML) method

described in reference 6 assuming no external noise. The corresponding cost function has the form

$$J_{\mathrm{ML}} = \sum_{i=1}^{N} \sum_{j=1}^{k} \frac{1}{\hat{\sigma}_j^2} \left[z_j(i) - \hat{z}_j(i, \hat{\Theta}) \right]^2 \qquad (2)$$

where k is the number of output variables, $\hat{\sigma}_j^2$ is the variance estimate of measurement noise, z_j and $\hat{z}_j$ are the measured and computed outputs, respectively, and $\hat{\Theta}$ is a vector of estimates of unknown parameters.

In addition to the parameter estimates, the ML method provides an estimate of the accuracy of each parameter through an approximation to the Cramer-Rao bound for that parameter. Theoretically, the Cramer-Rao bound presents a lower bound for the variance of the estimates of a parameter. The approximation to the Cramer-Rao bound is realized by the diagonal elements of the inverse of the Fisher information matrix. Since with flight data there is no "true" value with which to compare parameter estimates, agreement between the estimates of a given parameter from the ML and SR algorithms increases the overall confidence in that estimated value.

Results and Discussion

Data Compatibility

Three maneuvers that were designed specifically for a longitudinal data-compatibility check were analyzed using the algorithm developed in reference 7. This compares measured and predicted aircraft responses using the kinematic equations as a model. It employs the maximum likelihood technique for finding uncorrected systematic errors in measured responses in terms of constant bias errors and scale-factor errors. For the symmetric longitudinal maneuvers, possible biases in angle of attack (b_α), pitch rate (b_q), pitch angle (b_θ), longitudinal acceleration (b_{ax}), and vertical acceleration (b_{az}) were estimated. The resulting values are found in table II. In addition to the six bias values estimated, a scale factor in angle of attack (λ_α) was determined as a correction for upwash at the tip of the nose boom. Although computed angle-of-attack time histories appeared to correspond well with those measured in flight, the differences between measured and computed data (residuals) still exhibited a definite structure (were not randomly distributed). (See fig. 4.) As a possible remedy for this situation, several candidate time shifts were introduced in the angle-of-attack time histories. It was postulated that this action might account for an uncorrected lag present in the data recording technique or in effects of the dynamics of the vane. Although increasing time shifts did "whiten" residuals, there was no physical justification for corrections of the magnitude of shift required.

Because of these problems involving angle-of-attack values and an overall inconsistency in computed bias values for the three compatibility runs, the 45 repeated longitudinal maneuvers and 3 additional large-amplitude maneuvers were analyzed using the algorithm mentioned above. From the analysis of these maneuvers, mean values of upwash correction ($\bar{\lambda}_\alpha$) and all bias terms were compiled (table III).

The magnitude and consistency of bias values obtained from analyzing all runs gave sufficient confidence in the data acquisition system for the small perturbation maneuvers exciting the short-period modes of the aircraft. They were not used as corrections to the data because of their very low values and relatively high standard errors, a result which indicates that no real biases exist.

The average scale-factor estimate for upwash correction from the 45 repeat maneuvers was

$$\bar{\lambda}_\alpha = 0.10605$$

with the Cramer-Rao bound estimate of

$$\bar{s}(\lambda_\alpha) = 0.00660$$

and an ensemble standard deviation of

$$s_E(\lambda_\alpha) = 0.00741$$

The upwash correction was made to all measured α in the following manner:

$$\alpha_M = (1 + \lambda_\alpha)\alpha$$

or

$$\alpha = (1 + \lambda_\alpha)^{-1}\alpha_M$$

where α_M is the experimentally measured angle of attack and α is the corrected free-stream angle of attack.

Accuracy of Derivative Estimates

The purpose of executing the 45 maneuvers under identical flight conditions was to acquire a series of flight data sets that would yield a statistically significant base of parameter and error estimates. The benefits of such an ensemble are twofold. First, the standard error calculated for the ensemble of parameter estimates themselves gives us a measure of the

effectiveness of the maneuvers through the repeatability of the predicted parameters. Second, the comparison of the average standard errors obtained from the computer programs with the standard error for the ensemble gives us a sense of how realistic the program values are.

The 45 repeat maneuvers were analyzed using both the linear regression and the maximum likelihood methods, and the resulting mean values of coefficients are compiled in table IV. Accompanying each parameter estimate is the average standard error associated with it as given by the particular estimation algorithm, the standard error for the ensemble of values, and the ratio of the two. The ratio given for each parameter is the factor by which the program-estimated standard error for that parameter should be multiplied to produce a realistic, expected standard error. The ratios from the maximum likelihood results are seen to be greater than those from the linear regression. Two reasons are postulated for this difference: First, the standard error for each ML estimate is given by a numerical approximation to the Cramer-Rao bound. Theoretically, the Cramer-Rao bound for an estimated parameter represents the best achievable accuracy for that parameter. The approximation to the Cramer-Rao bound used in the algorithm that produced the ML parameter estimates presented in this paper is given by the diagonal elements of the inverse of an approximation to the Fisher information matrix. In general, for actual flight data, these theoretical values are smaller than the estimated standard error from an SR algorithm. This gives, in general, smaller numbers in the denominators for the maximum likelihood ratios as compared with the linear regression ratios. Second, the dispersion of values for the maximum likelihood estimates from these data was large for some parameters (C_{z_q} and $C_{z_{\delta_e}}$, in particular). This type of dispersion is usually due to multiple correlations among variables in the data and unmodeled dynamics (such as those giving rise to the structure of the angle-of-attack residuals discussed in the section on data compatibility).

All further analysis of flight data was principally carried out using the linear regression method because of the consistency of results obtained through it, whereas some comparison estimates were made using the maximum likelihood method.

Effects of Artificial Ice Shape

Following the 45 repeat maneuvers completed with the aircraft in each of the 4 configurations, the pilot executed several additional longitudinal doublets at varying initial airspeeds (ranging from 62 to 120 knots). These data were analyzed with the linear regression and maximum likelihood algorithms to study the variations of parameters with initial flight condition and between different configurations. The results obtained from the stepwise regression routine are presented graphically in figures 5 through 8. In no case did the stepwise regression select a nonlinear term as a component of the aerodynamic model.

Each parameter value is plotted with $\pm 2\sigma$ error bars, based on the standard error as given by the computer program. For the two configurations in which the flaps were held at 0°, there are statistically significant differences between iced and uniced flights. These differences generally decrease with increasing velocity. When the flaps are extended and held at 10°, however, the distinction between iced and uniced becomes less dramatic. Disturbances in the flow coming off the wings caused by the extended flaps appear to negate a large percentage of the effects of artificial ice attached to the leading edge of the tail section. The pitching-moment derivatives indicate that the artificial ice shape induces a loss of elevator effectiveness ($C_{m_{\delta_e}}$), a decrease in static stability (C_{m_α}), and lower pitch damping (C_{m_q}).

Derivative values obtained from selected maneuvers using the maximum likelihood routine are presented in figure 9. Because of the convergence problems mentioned earlier, the maximum likelihood algorithm was run only on several selected maneuvers. The resulting values were usually in agreement with the regression-determined parameters with respect to trends, but they differed significantly in actual values estimated. No reason was found for those differences.

Error Analysis

A fundamental issue throughout this research is that of distinguishing between the effects of ice and the inherent variability of predicted parameters. In addition to the error analysis performed on the values obtained from the 45 repeat maneuvers, the $C_{m_{\delta_e}}$ estimates for the 0° flap condition were considered (fig. 10) for an additional analysis. This set of points was chosen for this portion of the analysis because each of the two groups of values (iced and uniced) lend themselves to linear approximations. Also, determining a prediction interval (denoted by the terms in brackets) in this particular case serves to quantitatively enforce what is qualitatively a very noticeable difference in parameters for the iced/uniced cases. After approximating the two groups of points by straight lines, prediction intervals about these lines

were calculated as follows:

$$[y_0(x_0)] + \left[t_{\alpha*/2,n-2}\right] \times s \left[1 + n^{-1} + (x_0 - x)^2 / S_{XX}\right]^{1/2} \quad (3)$$

where

$y_0(x_0)$	linear approximation of $C_{m_{\delta_e}}$ corresponding to some x_0 value
α^*	0.05 to achieve a 95-percent prediction interval
n	number of data points
$t_{\alpha*/2,n-2}$	student t-distribution
s	standard error (can be one of three substitutions listed below):
$s_{PA}(y)$	average of standard errors obtained from computer program
$s_E(y)$	ensemble-average standard error for values of $C_{m_{\delta_e}}$, $\left[\sum(y_i - y)^2/(n-2)\right]^{1/2}$
$s_R(y)$	$s_{PA}(y)$ multiplied by ratio of ensemble to program average obtained from table IV
S_{XX}	sum of squares of residuals, $\sum_{i=1}^{N}(x_i - \bar{x})^2$

The resulting interval is one within which we can expect 95 percent of all predicted elevator-effectiveness values to fall. Figure 10 presents these prediction intervals and gives an illustration of both the areas in which icing effects are discernible as well as the speed range in which we cannot attribute any change in $C_{m_{\delta_e}}$ to the artificial ice shape. A similar analysis can be done on other parameters by fitting them in a piecewise linear fashion.

Conclusions

Based on the analysis and results presented, the following four basic conclusions are presented:

1. Any future research of this type will require determination of the cause of error found in angle-of-attack measurements.

2. A multiplicative relationship between ensemble standard error and estimated standard error from the stepwise regression routine was identified with numerical values representing this ratio assigned to each stability and control derivative.

3. A multiplicative relationship between ensemble standard errors and those obtained as an approximation to the Cramer-Rao bound as given by the maximum likelihood program was determined as a quantitative ratio for each parameter estimated.

4. The effects of the artificial ice shape attached to the tail section have been shown to be measurable as changes in the longitudinal stability and control derivatives in all the flight test conditions addressed here with the largest effects being seen in those derivatives most directly determined by the flow on the tail, i.e., static stability (C_{m_α}), pitch damping (C_{m_q}), and elevator effectiveness ($C_{m_{\delta_e}}$).

NASA Langley Research Center
Hampton, VA 23665-5225
January 25, 1989

Appendix

Postulated Models

The six-degrees-of-freedom equations of motion for the aircraft are

$$\dot{u} = -qw + rv - g \sin\theta + \frac{\rho V^2 S}{2m} C_X \tag{4}$$

$$\dot{v} = -ru + pw + g \cos\theta \sin\phi + \frac{\rho V^2 S}{2m} C_Y \tag{5}$$

$$\dot{w} = -pv + qu + g \cos\theta \cos\phi + \frac{\rho V^2 S}{2m} C_Z \tag{6}$$

$$\dot{p} = qr\left(\frac{I_Y - I_Z}{I_X}\right) + \frac{I_{XZ}}{I_X}(pq + \dot{r}) + \frac{\rho V^2 Sb}{2I_X} C_l \tag{7}$$

$$\dot{q} = pr\left(\frac{I_Z - I_X}{I_Y}\right) + \frac{I_{XZ}}{I_Y}(r^2 - p^2) + \frac{\rho V^2 S\bar{c}}{2I_Y} C_m \tag{8}$$

$$\dot{r} = pq\left(\frac{I_X - I_Y}{I_Z}\right) + \frac{I_{XZ}}{I_Z}(\dot{p} - qr) + \frac{\rho V^2 Sb}{2I_Z} C_n \tag{9}$$

along with the kinematic relations

$$\dot{\theta} = q \cos\phi - r \sin\phi \tag{10}$$

and

$$\dot{\phi} = p + (q \sin\phi + r \cos\phi)\tan\theta \tag{11}$$

Here, equations (4), (6), (8), and (10) describe the longitudinal motion and equations (5), (7), (9), and (11) describe the lateral motion of the aircraft. The angles of attack and sideslip are, respectively, given by

$$\alpha = \tan^{-1}(w/u) \qquad \beta = \sin^{-1}(v/V)$$

The aerodynamic forces and moments are represented by the coefficients C_a (where $a = X, Y, Z, l, m,$ or n). It is postulated that these coefficients can be written as a Taylor-series polynomial expansion about an equilibrium trim condition as

$$C_a = \Theta_{a,0} + \sum_{j=1}^{\ell} \Theta_{a,j} \, \Delta x_j \tag{12}$$

where $\Theta_{a,0}$ and $\Theta_{a,j}$ are the unknown parameters. For $a = X, Z,$ or m, the independent variables x_j are α, $q\bar{c}/2V$, δ_e, and their combinations; and for $a = Y$, l, or n, they are β, $pb/2V$, $rb/2V$, δ_a, δ_r, and their combinations. Furthermore,

$$\Delta x_j = x_j(t) - x_j \qquad (t = 0)$$

References

1. *Federal Coordinator for Meteorological Services and Supporting Research: National Aircraft Icing Technology Plan.* FCM-P20-1986, Dep. of Commerce, Apr. 1986.
2. Ranaudo, Richard J.; Mikkelsen, Kevin L.; McKnight, Robert C.; Ide, Robert F.; Reehorst, Andrew L.; Jordan, Jerry L.; Schinstock, William C.; and Platz, Stewart J.: The Measurement of Aircraft Performance and Stability and Control After Flight Through Natural Icing Conditions. AIAA-86-9758, Apr. 1986.
3. Jordan, Jerry L.; Platz, Stewart J.; and Schinstock, William C.: *Flight Test Report of the NASA Icing Research Airplane—Performance, Stability, and Control After Flight Through Natural Icing Conditions.* NASA CR-179515, 1986.
4. Maine, Richard E.; and Iliff, Kenneth W.: *Application of Parameter Estimation to Aircraft Stability and Control—The Output-Error Approach.* NASA RP-1168, 1986.
5. Batterson, James G.: *STEP and STEPSPL—Computer Programs for Aerodynamic Model Structure Determination and Parameter Estimation.* NASA TM-86410, 1986.
6. Murphy, Patrick C.: *An Algorithm for Maximum Likelihood Estimation Using an Efficient Method for Approximating Sensitivities.* NASA TP-2311, 1984.
7. Klein, Vladislav; and Morgan, Dan R.: *Estimation of Bias Errors in Measured Airplane Responses Using Maximum Likelihood Method.* NASA TM-89059, 1987.
8. Klein, Vladislav; Batterson, James G.; and Murphy, Patrick C.: *Determination of Airplane Model Structure From Flight Data by Using Modified Stepwise Regression.* NASA TP-1916, 1981.

Table I. Physical Characteristics of Research Aircraft

	Low	High
Mass, kg	4150	4600
Inertia:		
I_X, kg-m^2	21 300	21 790
I_Y, kg-m^2	30 000	31 030
I_Z, kg-m^2	44 990	48 640
I_{XZ}, kg-m^2	1430	1500
Wing:		
Area, m^2		39.02
Aspect ratio		10.06
Span, m		19.81
Mean geometric chord, m		1.98
Airfoil section (17-percent thickness)		"deHavilland High Lift"
Horizontal tail:		
Area, m^2		9.1
Airfoil section (inverted)		NACA 63A213

Table II. Estimated Bias and Scale-Factor Errors Present in Longitudinal-Data Compatibility Maneuvers for Flight 88-5

Estimated parameter	Longitudinal compatibility maneuvers for—		
	Run 33	Run 34	Run 35
b_α, rad	0.0038 ± 0.0006	0.0092 ± 0.0007	−0.0047 ± 0.0007
b_q, rad/sec	0.00057 ± 0.00003	0.000996 ± 0.2E−09	0.000645 ± 0.3E−07
b_θ, rad	−0.0175 ± 0.0005	−0.0173 ± 0.0003	−0.0207 ± 0.0004
b_{ax}, g units	0.123 ± 0.003	0.089 ± 0.030	0.002 ± 0.002
b_{az}, g units	0.014 ± 0.001	0.004 ± 0.002	−0.056 ± 0.001
λ_α	0.022 ± 0.005	−0.054 ± 0.008	0.128 ± 0.010

Table III. Estimated Bias and Scale-Factor Errors Present in Longitudinal Doublets and Large-Amplitude Maneuvers for Flight 88-5

Estimated parameter	Average of 45 repeat maneuvers	Large-amplitude maneuvers for—		
		Run 36	Run 37	Run 38
b_α, rad	−0.00324 ± 0.00092	0.000598 ± 0.0019	0.00176 ± 0.0023	−0.00381 ± 0.00232
b_q, rad/sec	0.00044 ± 0.000488	0.00181 ± 0.00016	0.000829 ± 0.00013	0.00129 ± 0.000151
b_θ, rad	0.00040 ± 0.00156	−0.00618 ± 0.00261	−0.0189 ± 0.0023	−0.0131 ± 0.00253
b_{ax}, g units	0.0353 ± 0.01606	−0.00288 ± 0.0164	−0.0629 ± 0.0150	−0.0144 ± 0.0163
b_{az}, g units	0.00339 ± 0.0285	−0.0837 ± 0.00561	−0.0528 ± 0.00682	−0.0875 ± 0.00717
λ_α	0.10605 ± 0.00660	0.0819 ± 0.0142	0.1049 ± 0.0255	0.1132 ± 0.0227

Table IV. Mean Values of Stability and Control Derivatives Calculated From the 45 Repeat Maneuvers

(a) Linear regression

Parameter	$\overline{\Theta}$ (a)	Standard errors		$s_E(\Theta)/s(\Theta)$
		$s_E(\Theta)$ (b)	$s(\Theta)$ (c)	
C_{Z_α}	−5.66	0.0493	0.0169	2.9
C_{Z_q}	−19.97	1.047	.386	2.7
$C_{Z_{\delta_e}}$	−.608	.0281	.0122	2.3
C_{m_α}	−1.31	.0147	.0191	.8
C_{m_q}	−34.2	.6444	.4314	1.5
$C_{m_{\delta_e}}$	−1.74	.0248	.0131	1.9

(b) Maximum likelihood

Parameter	$\overline{\Theta}$ (a)	Standard errors		$s_E(\Theta)/s(\Theta)$
		$s_E(\Theta)$ (b)	$s(\Theta)$ (c)	
C_{Z_α}	−5.28	0.3763	0.1933	1.9
C_{Z_q}	−2.00	17.4	.444	39.3
$C_{Z_{\delta_e}}$	−.039	.8457	.1264	6.7
C_{m_α}	−1.42	.116	.0272	4.3
C_{m_q}	−41.3	10.33	.4416	23.4
$C_{m_{\delta_e}}$	−1.97	.180	.0386	4.7

[a] Mean value of Θ.
[b] $s_E(\Theta)$: ensemble standard error.
[c] $s(\Theta)$: average program standard error.

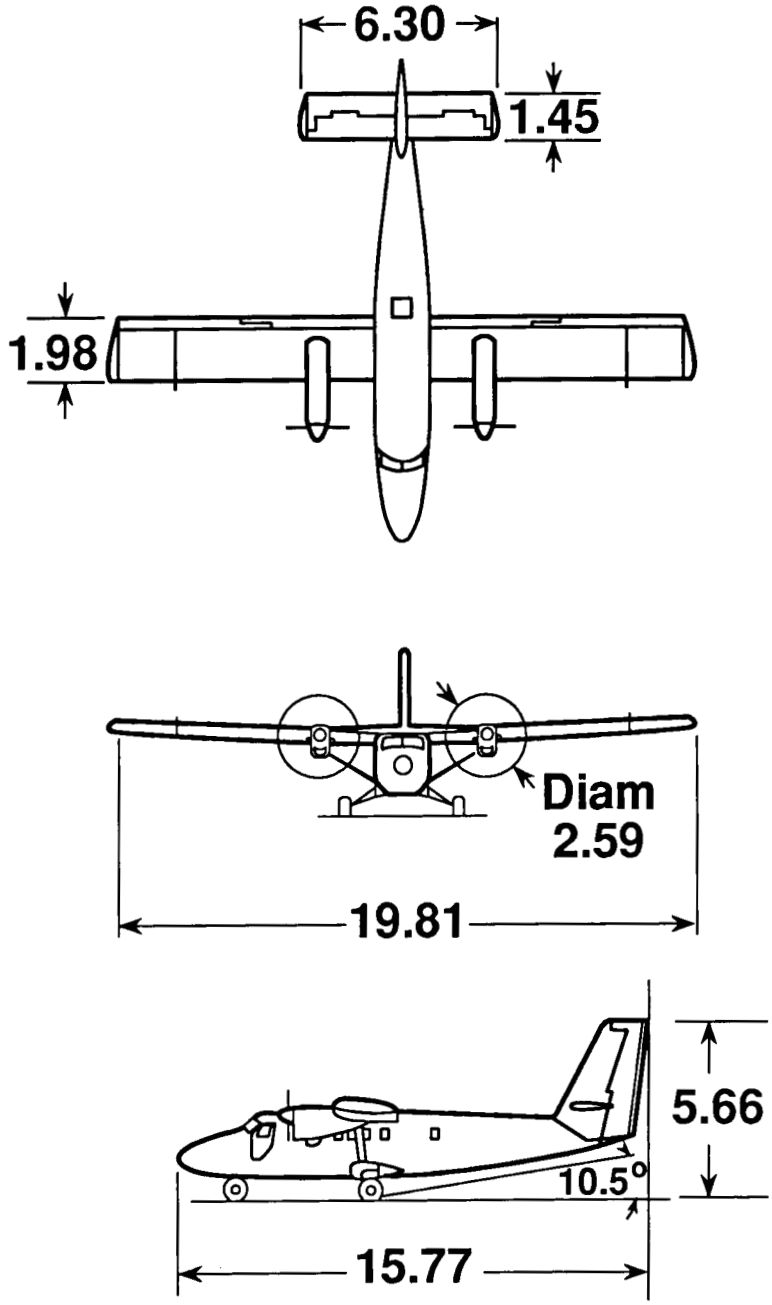

Figure 1. Three-view drawing of icing research aircraft.

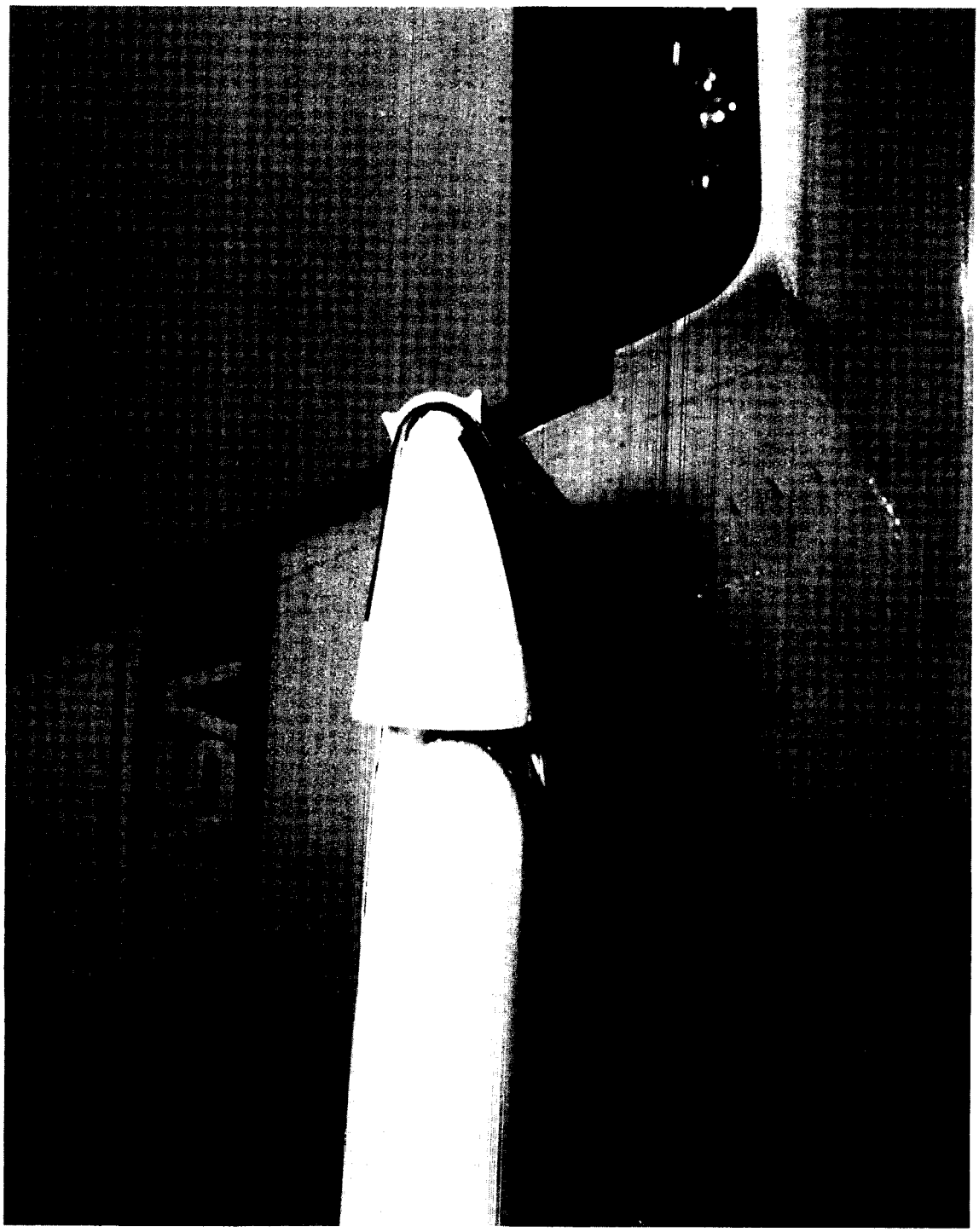

C-85-4763

Figure 2. Artificial glaze-ice form in place of horizontal tail.

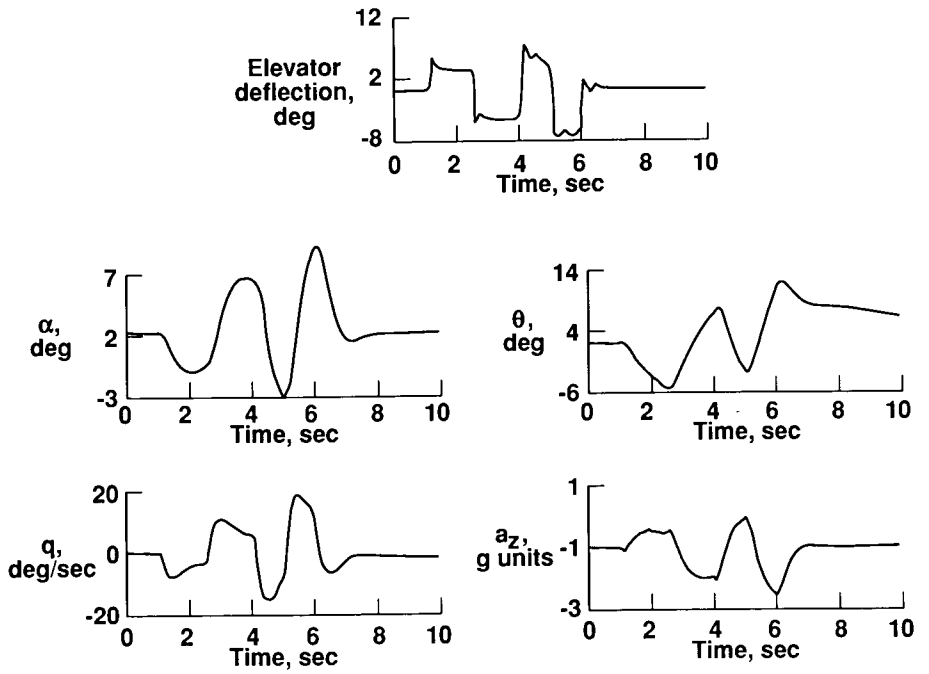

Figure 3. Control surface input and aircraft response for typical 2-1 elevator doublet.

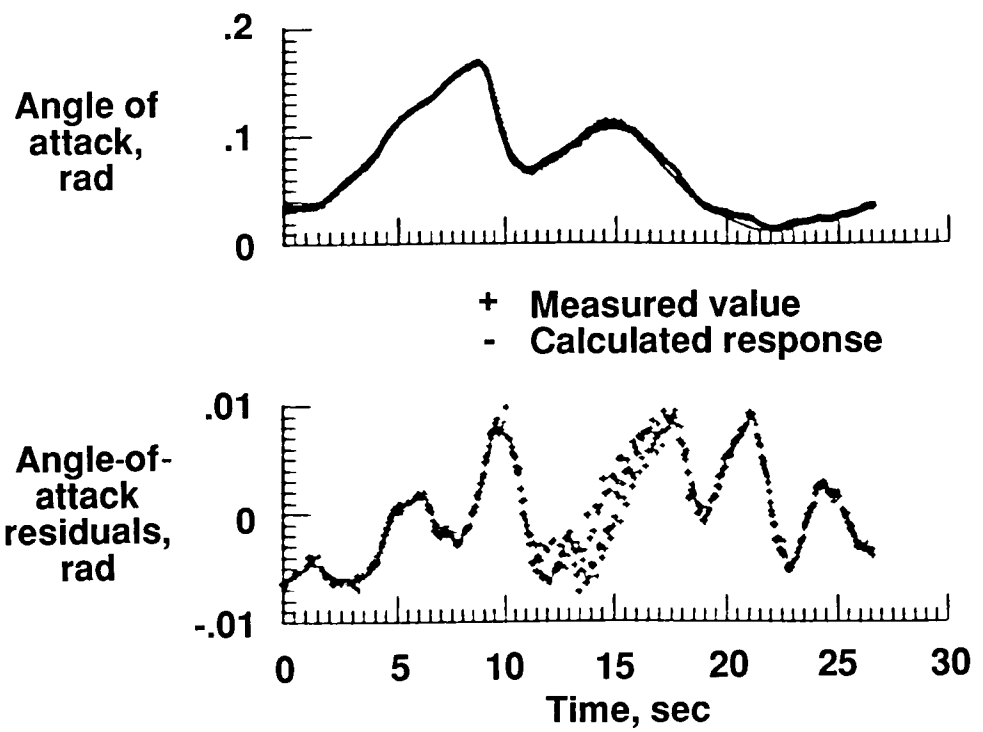

Figure 4. Results from compatibility check on angle of attack.

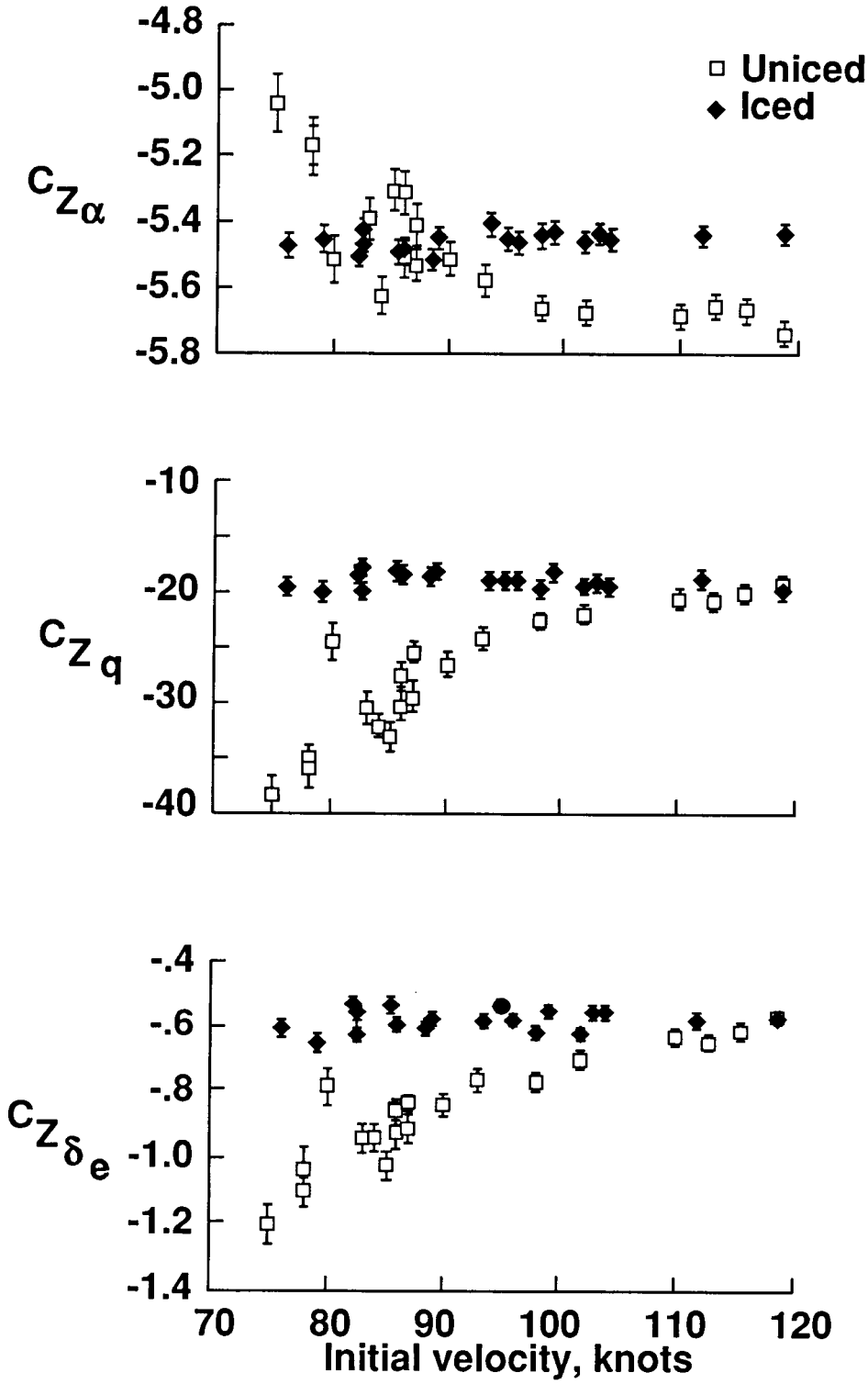

Figure 5. Vertical force derivatives and $\pm 2\sigma$ error bounds from modified stepwise regression for flaps at 0°.

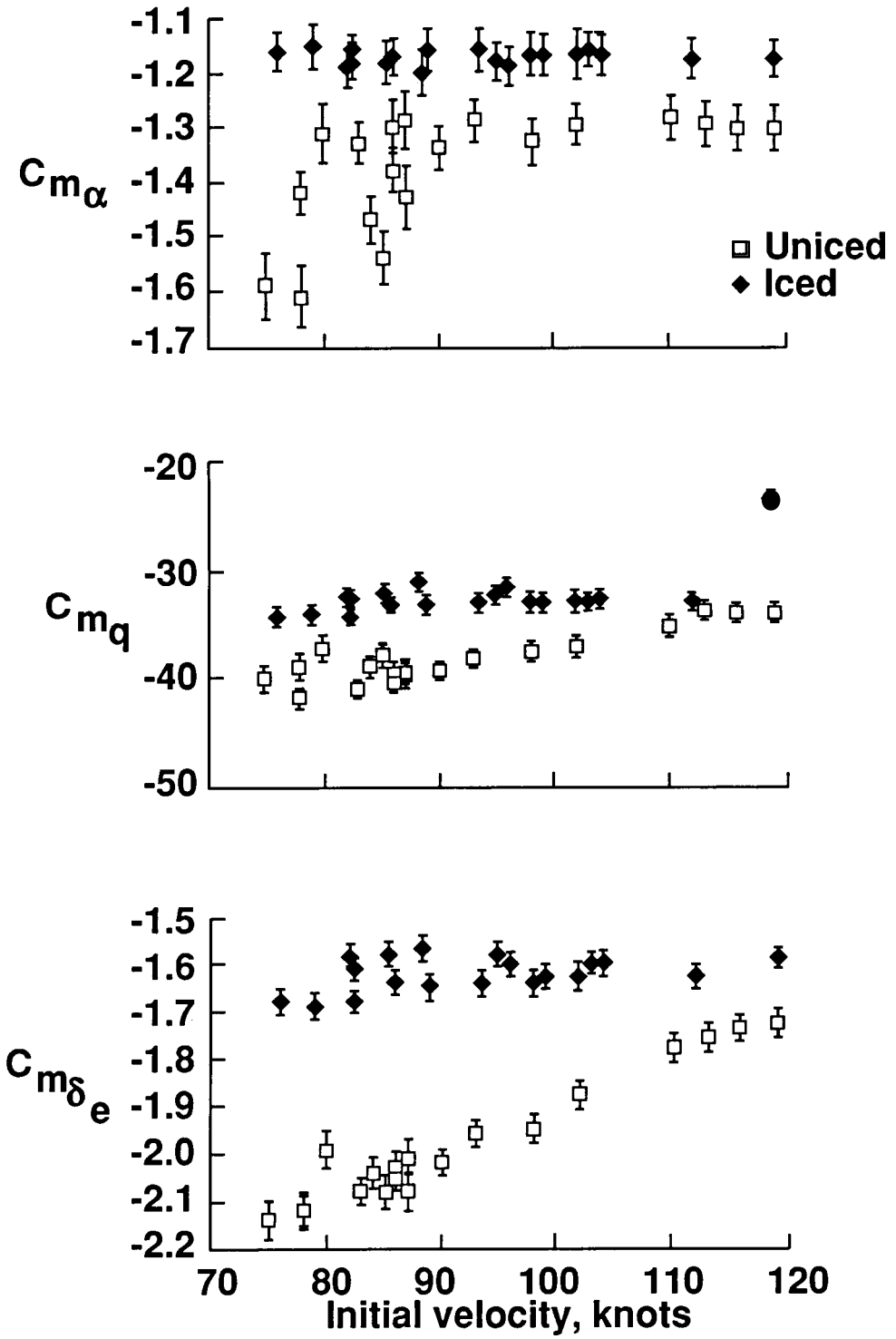

Figure 6. Pitching-moment derivatives and $\pm 2\sigma$ error bounds from modified stepwise regression for flaps at 0°.

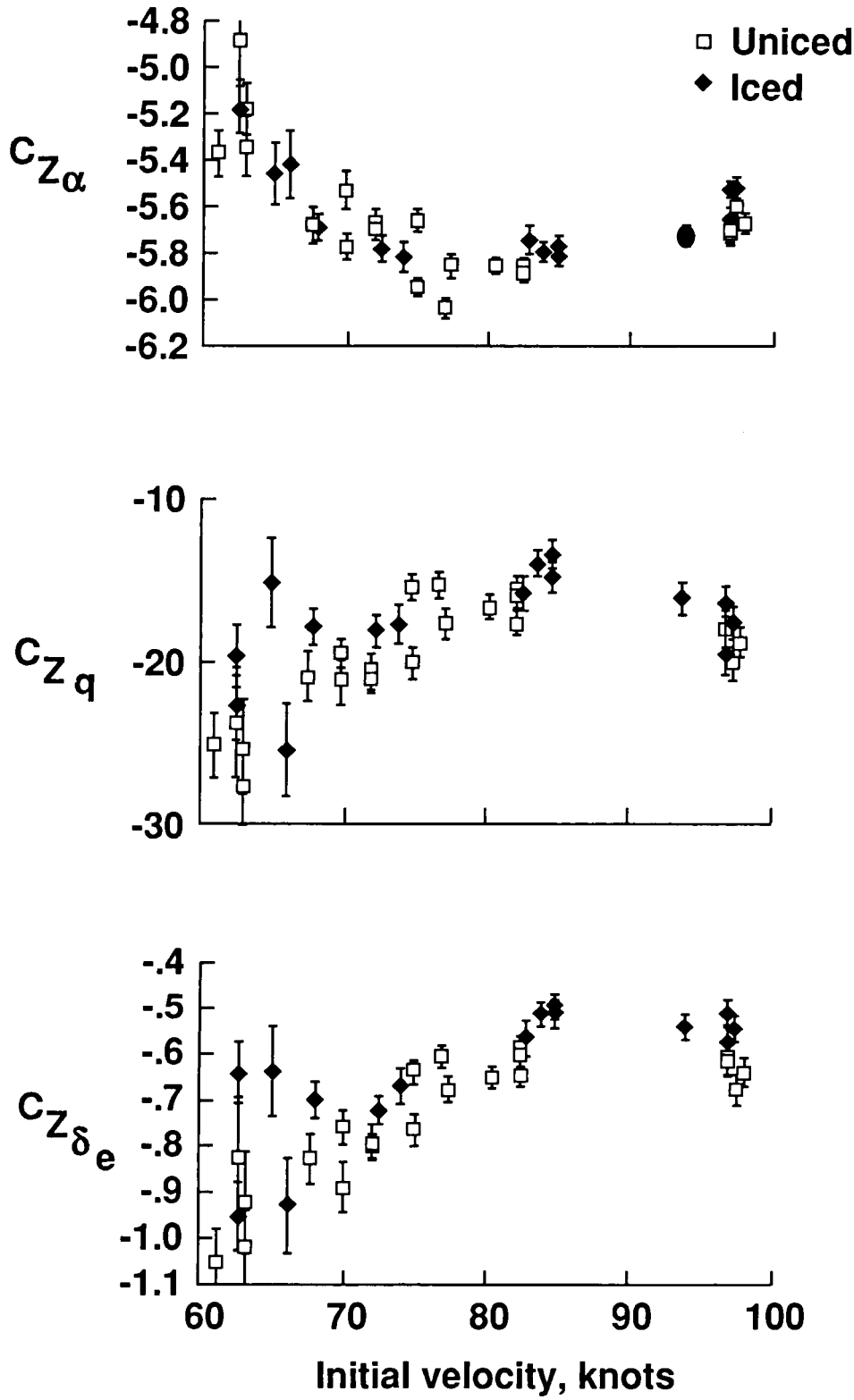

Figure 7. Vertical force derivatives and $\pm 2\sigma$ error bounds from modified stepwise regression for flaps at 10°.

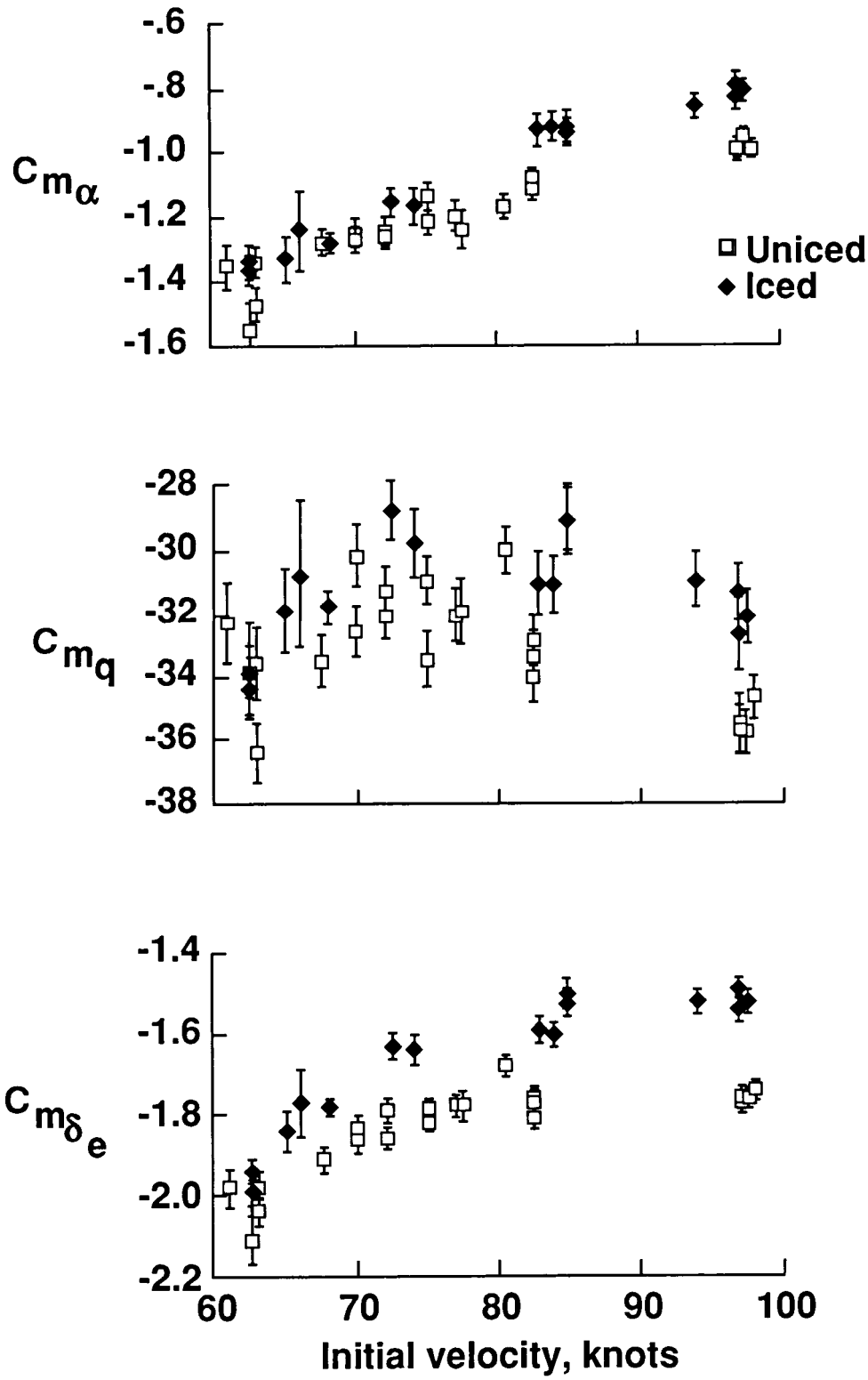

Figure 8. Pitching-moment derivatives and $\pm 2\sigma$ error bounds from modified stepwise regression for flaps at 10°.

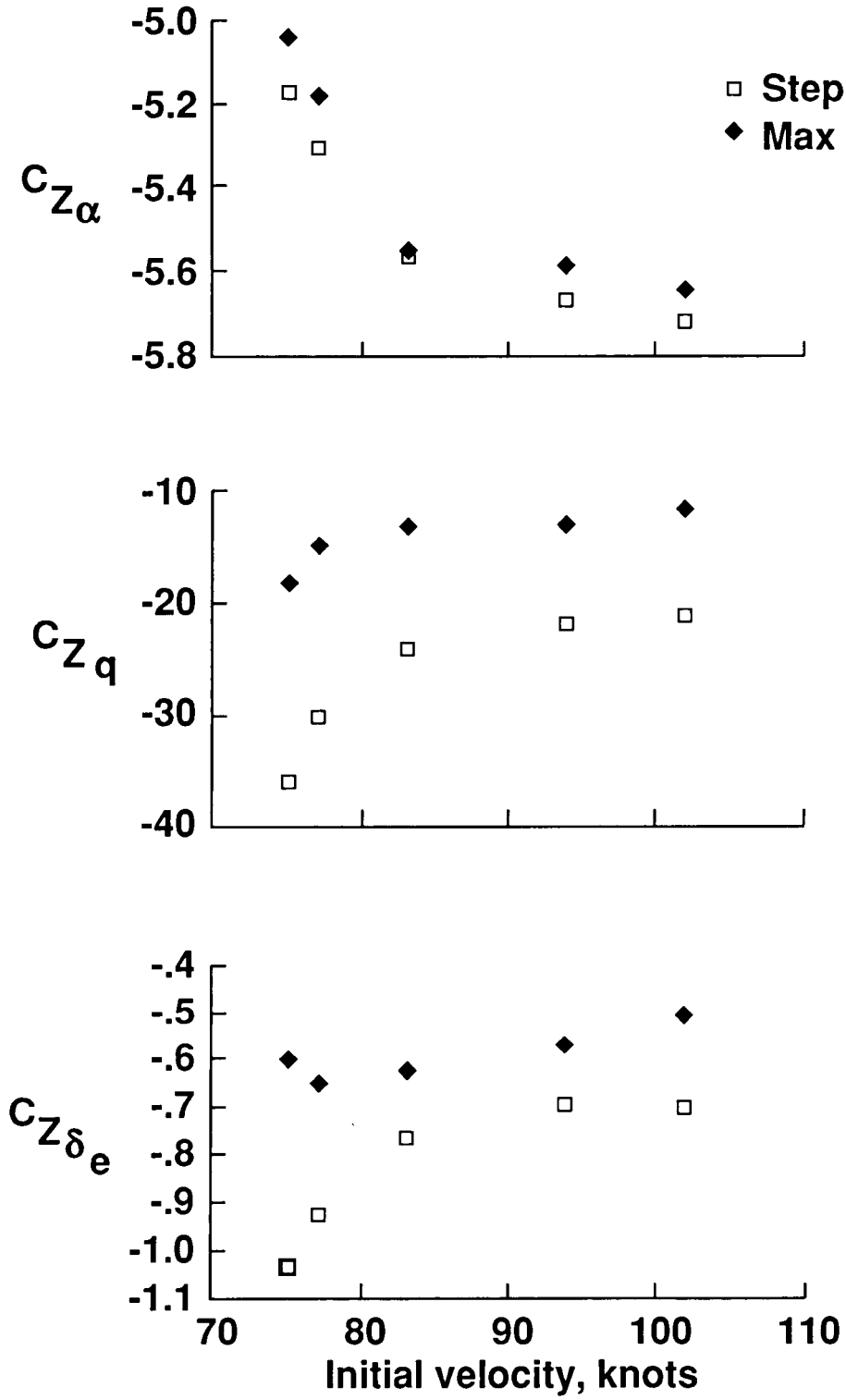

Figure 9. Comparison of modified stepwise regression results with maximum likelihood results. Clean aircraft; flaps at 0°.

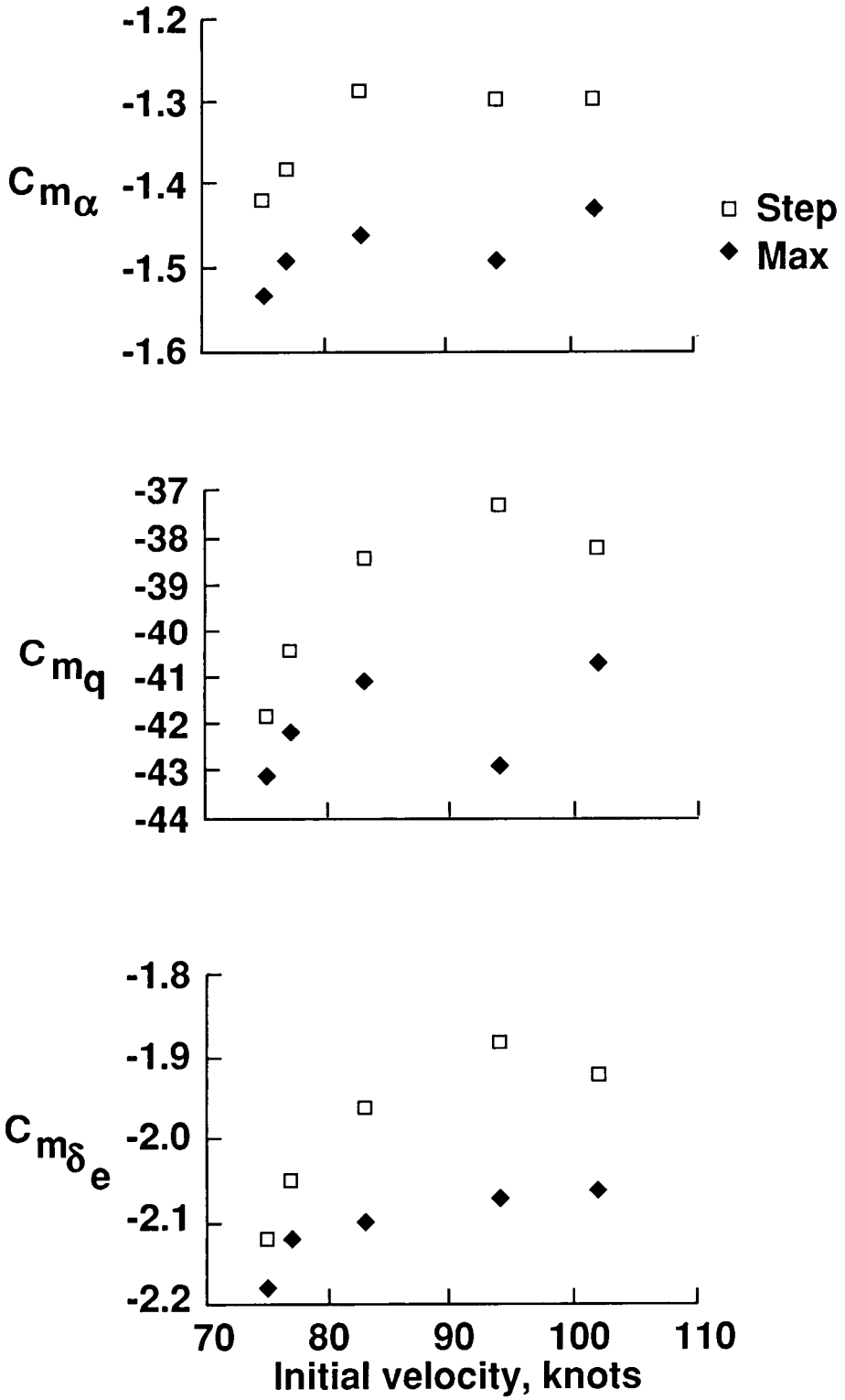

Figure 9. Concluded.

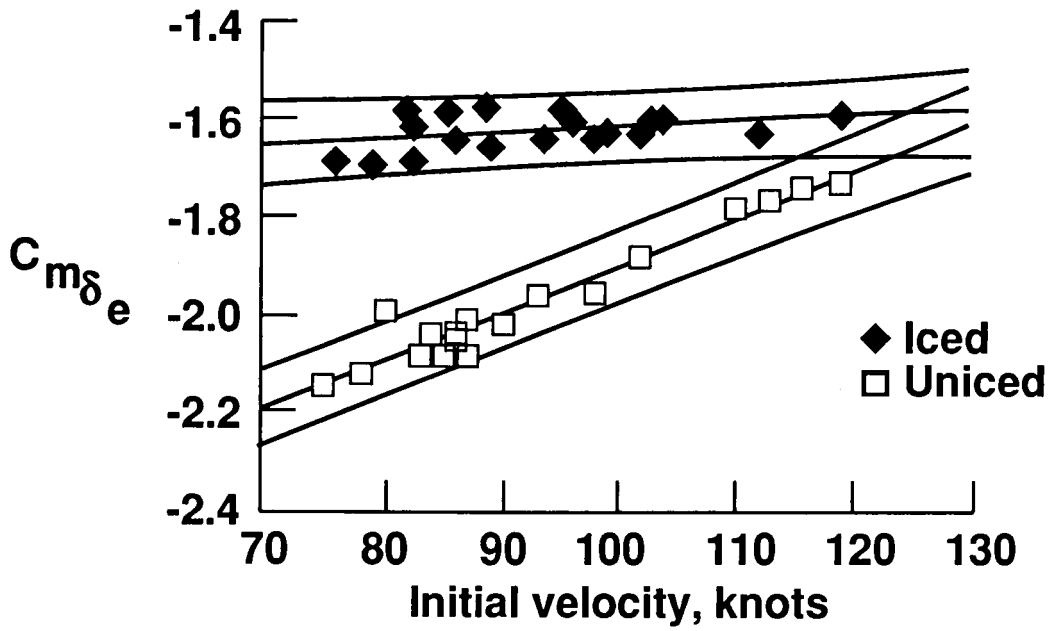

Figure 10. Confidence intervals of 95 percent for elevator-effectiveness derivatives for iced and uniced aircraft.

NASA
National Aeronautics and Space Administration

Report Documentation Page

1. Report No.	2. Government Accession No.	3. Recipient's Catalog No.
NASA TM-4099		

4. Title and Subtitle	5. Report Date
Estimation of Longitudinal Stability and Control Derivatives for an Icing Research Aircraft From Flight Data	March 1989
	6. Performing Organization Code
7. Author(s)	8. Performing Organization Report No.
James G. Batterson and Thomas M. O'Mara	L-16478
9. Performing Organization Name and Address	10. Work Unit No.
NASA Langley Research Center Hampton, VA 23665-5225	505-66-01-02
	11. Contract or Grant No.
12. Sponsoring Agency Name and Address	13. Type of Report and Period Covered
National Aeronautics and Space Administration Washington, DC 20546-0001	Technical Memorandum
	14. Sponsoring Agency Code

15. Supplementary Notes

James G. Batterson: Langley Research Center, Hampton, Virginia.
Thomas M. O'Mara: The George Washington University, Joint Institute for Advancement of Flight Sciences, Langley Research Center, Hampton, Virginia.

16. Abstract

The National Aeronautics and Space Administration, at its Lewis Research Center, develops and coordinates plans and results related to icing computer-code predictions, icing research tunnel (IRT) measurements, and icing research flights. To allow for the comparison of research flight results with icing code predictions and IRT measurements, Lewis has collaborated with the NASA Langley Research Center for the planning and analysis of a series of icing research flights related to the determination of stability and control derivatives from research flight data. This paper presents the results of applying a modified stepwise regression algorithm and a maximum likelihood algorithm to flight data from a twin-engine commuter-class icing research aircraft. The results are in the form of body-axis stability and control derivatives related to the short-period, longitudinal motion of the aircraft. Data were analyzed for the baseline aircraft ("uniced") and for the aircraft with an artificial glaze-ice shape attached to the leading edge of the horizontal tail. The results are discussed as to the accuracy of the derivative estimates and the difference between the derivative values found for the baseline and the "iced" aircraft. Additional comparisons are made between the maximum likelihood results and the modified stepwise regression results with causes for any discrepancies postulated.

17. Key Words (Suggested by Authors(s))	18. Distribution Statement
Icing System identification Stepwise regression Cramer-Rao bounds Aircraft stability and control	Unclassified—Unlimited Subject Category 08

19. Security Classif. (of this report)	20. Security Classif. (of this page)	21. No. of Pages	22. Price
Unclassified	Unclassified	22	A03

For sale by the National Technical Information Service, Springfield, Virginia 22161-2171